Electronic version of an article published as Innovation and Emerging Technologies, 10, 2340005, 2024 https://doi.org/10.1142/S2737599423400054 © copyright World Scientific Publishing Company https://www.worldscientific.com/worldscinet/iet

A robust, flow-based, microfluidic device for siRNA mediated gene knockdown in glioblastoma spheroids

Authors: Ines Hosni[1], Alex Iles[2], John Greenman[1] and Mark A Wade[1a]

Affiliation:

[1] Centre for Biomedicine, Hull York Medical School, University of Hull, Hull HU6 7RX, UK.

[2] Department of Materials and Environmental Chemistry, Stockholm University, Svante Arrhenius väg 16 C, 106 91 Stockholm, Sweden.

[a] Author to whom correspondence should be addressed: mark.wade@hyms.ac.uk

Abstract

Glioblastoma (GBM) is a deadly disease with a poor prognosis, there is therefore a crucial need for novel therapeutic targets. Current preclinical models of GBM fail to predict clinical outcomes, thus new translationally relevant models are urgently needed for reliable therapeutic target validation. 3D spheroid culture of cancer cells has been shown to better reflect tumour biology than 2D monolayer culture, as has culturing cells in flow-based microfluidic devices which mimic key aspects of the tumour microenvironment. Gene knockdown by siRNA is a key preclinical target validation tool, however siRNA mediated knockdown of cancer spheroids in microfluidic culture has not yet been demonstrated. Here we describe a simple and robust microfluidic device that can maintain GBM spheroids (U87 cells) for at least 7 days. Via RNA-sequencing analysis we demonstrate that spheroids grown in microfluidic culture are more proliferative than spheroids grown in static plate culture and downregulate genes associated with cell adhesion, potentially offering insights into the metastatic process. Comparison of target gene (*PRMT2* and *RAB21*) knockdown using siRNA between 2D monolayer cultured cells, static spheroid culture and spheroids maintained in the microfluidic device showed that gene expression (as measured by quantitative-PCR) was significantly reduced in all culture systems. Knockdown was most efficient in cells grown in 2D monolayer culture followed by static spheroid culture, but we also demonstrate ~40% knockdown efficiency using the microfluidic device. In summary, this study describes an easy to use microfluidic culture platform and provides evidence that pre-clinical siRNA mediated target validation studies will be possible in flow systems that mimic tumour physiology.

Introduction

Glioblastoma multiforme (GBM) is a grade IV astrocytoma tumour which is highly proliferative and accounts for around half of all diagnosed malignant primary brain tumours [1, 2]. GBM is a particularly aggressive form of brain tumour with poor prognosis and only a 5-year survival rate around 5.5% and median survival of 15 months[2]. For newly diagnosed GBM patients the effective standard of care is surgical resection followed by concomitant radiotherapy and treatment with temozolomide [2, 3]. Due to the invariably invasive nature of the tumour, surgical resection and adjuvant chemo-radiation is often not curative, with recurrence of the disease occurring in approximately 80% of cases. Recurrence usually occurs within 2-3 cm of the margin of the original lesion and within 10 months of treatment being completed[4]. Additionally, after prolonged use of TMZ the activity of the drug is reduced and patients who initially responded to TMZ develop resistance and inevitably relapse[5]. Despite extensive research for new therapeutic approaches the prognosis of the disease has not improved drastically in the last 20 years, with very few proposed therapeutic targets reaching the clinic[6, 7].

RNA-interference (RNAi) technology, which utilises specifically designed double stranded RNA sequences to knock down expression of target genes and hence proteins via the cells own natural post-translational gene silencing mechanisms, has been an extremely useful tool to assess the functionality of potential therapeutic targets in cancer[8]. The use of small interfering RNA (siRNA) and short hairpin RNA (shRNA) sequences to knock down target genes have been used for many years in high-throughput target identification screens to identify genes that are required for cancer cell survival and growth, and genes that promote chemotherapeutic resistance[9, 10]. A key use of RNAi technology, however, is also for more targeted and detailed target validation studies of specific genes in cancer[9, 11-14]. The ability to deplete expression of specific genes in order to analyse multiple phenotypic and molecular biological outputs is a powerful way to elucidate gene and protein function. However, one of the roadblocks for therapeutic target validation studies using this technique in GBM is a lack of translationally relevant pre-clinical models[15]. Classically, primary or immortalised GBM cell lines have been used to investigate cancer mechanisms. These cells can be cultured as 2D monolayers or in 3D spheroid culture, often in static plastic culture conditions that have inherent translational limitations. For example, 2D cell culture models do not mimic the microenvironment of the tumour mass which limit their translational relevance for therapeutic target identification and validation. 2D culture models almost always comprise a single cell line which commonly lose their original phenotype, such as morphology and polarity, which results in changes in cell replication, function, organisation, structure and cell signalling[16]. Additionally, in contrast to *in vivo* conditions, where the availability of nutrients, oxygen and signalling molecules is variable among the 3D structure of the multiple cell types within a tumour mass, in a monolayer system, cells are under a continuous supply

of these elements without any removal of waste products[17]. 3D spheroids exhibit features more similar to *in-vivo* tumour tissues due to their multilayer structure which potentially makes them a more suitable tool for target validation studies compared to 2D monolayer cell cultures[18-20]. However, 3D spheroids also have similar limitations in relation to access to nutrients and lack of waste removal when grown in static plastic culture conditions. Due to the limitations of these cell based models the effect of genetic manipulation of promising therapeutic targets is often not replicated in an *in vivo* or *ex vivo* setting.

Microfluidic culture of GBM spheroids has removed some of the aforementioned limitations. Microfluidic devices can allow a continuous flow of defined nutrients across cells or tissue with a concomitant removal of waste products, thereby recreating some key features of human physiology[21, 22]. Accordingly, these models have been shown to mimic more closely the tumour microenvironment than 2D and 3D static culture systems and have led to innovative advances in cancer research[23-25].

To date there has been very little investigation into the utility of RNAi technology for gene function and target validation studies using microfluidic culture systems. Some success for gene knockdown in flowing platforms has been seen using primary fibroblasts and glial cells studying axon growth[26] and studying tumour angiogenesis using nanoparticle delivery of siRNA[27], however as a cancer target validation approach microfluidic culture and RNAi have not been combined. In this study we aimed to demonstrate that specific target gene knockdown of cancer cell spheroids is possible in a microfluidic platform and show the potential for future therapeutic target validation studies of specific targets in GBM. We describe a microfluidic chip for the maintenance of GBM spheroids and provide evidence that RNAi based functional genetic study using the model is possible. This was shown by comparisons of gene knockdown of cells grown in 2D monolayers, static spheroid culture in tissue culture plates, and spheroid culture using the microfluidic device. The ability to do functional gene studies on a more translationally relevant microfluidic platform to 2D culture will enhance the likelihood of identified targets being applicable *in vivo*, and would provide a key tool in therapeutic target validation for GBM and other solid malignancies.

Materials and Methods

Cell culture

The human glioblastoma cell line U87 was purchased from European Collection of Authenticated Cell Cultures (ECACC). Cell Line Authentication was carried out by short tandem repeat “fingerprinting” where the DNA Profile generated from the provided samples were compared to a profile located on

the Cellosaurus Database (NorthGene UK). The cell lines tested negative for any mycoplasma contamination and were retested every 6 months.

Cells were cultured in Dulbecco's Modified Eagle Medium (DMEM, Lonza, Castleford, UK) containing 25mM HEPES (Sigma, Gillingham, UK), 10% (v/v) foetal bovine serum (FBS, Gibco, Life Technologies, Loughborough, UK), penicillin/streptomycin for a final concentration of 100U/ml (Lonza, UK). To form spheroids cells were seeded at 2 x 10^4 cells/well in 100µl of medium in round-bottomed 96 well plate Ultra-Low Attachment (ULA) (Corning Costar, UK) as previously described[28]

Microfluidic chip setup

The microfluidic chips used in this work were made of the thermoplastic poly (methyl methacrylate) (PMMA). Each chip was composed of four separate pieces: the inlet piece, sample chamber, tissue retaining piece and outlet piece. These components were designed using AutoCAD software and then fabricated using a laser cutter (LS6840 Pro, HPC Laser, UK). The individual parts were assembled in the correct order and then solvent bonded by hand, using small quantities of chloroform The inlet and outlet parts were designed so that they could be interfaced with standard Luer to barb tubing connections. Before cell culture, chips were sterilised using 70% (v/v) ethanol and primed using sterile medium. Syringes (20ml) were filled with medium (volume depending on the experiment) and spheroids were collected from ULA plates and transferred to the device in a Class II biological safety cabinet before being placed in an egg incubator at 37°C. A 0.22µm syringe filter connected the syringe to the inlet tube of the chip, and an effluent collector (50 mL polypropylene tube) was connected to the outlet tube. The syringes were placed on an electronic syringe pump (Harvard Apparatus, PHD Ultra) which injected media through the chip at a flow rate of 2 µl/min[23].

siRNA transfection

siRNA transfections were performed on cells cultured as a 2D monolayer, or spheroids cultured in ULA plates (static culture) or in the microfluidic chip (flowing culture). Cells were transfected with either a *PRMT2* targeting siRNA (siPRMT2 - ON-TARGETplus Human siRNA, catalogue number L-004033-00-0010), *RAB21* targeting siRNA (siRAB21 - ON-TARGETplus Human siRNA, catalogue number L-009450-00-0010) or non-targeting control siRNA (siSCR - ON-TARGETplus Non-targeting Control siRNA, catalogue number D-001810-01-20). Transfection mixtures to achieve the experimental final concentration of siRNA (5nM – 25nM) were prepared according to the DharmaFECT siRNA transfection protocol. For monolayer culture U87 cells were transfected 24hr after seeding in 6 well plates while for spheroid transfections spheroids were first formed in ULA plates then transfected with siRNA either in the static or in the flow system.

Gene expression analysis

RNA was extracted from cells using TRIzol (Fisher Scientific, Loughborough, UK) following manufacturer's instructions. Spheroids were retrieved from the ULA plate or chip and transferred to RNAse free Eppendorf tubes (Fisher Scientific, UK) prior to the addition of 500µl of TRIzol™ reagent. cDNA was generated by reverse transcription from 1 µg of RNA for analysis by quantitative-PCR (qPCR). qPCR was performed using SYBR Green JumpStart TaqReady Mix (Merck, UK) and a StepOne Plus Real-Time PCR machine (Applied Biosystems, UK) (primer sequences in Supplementary Table S1). Gene expression relative to the siSCR control sample was calculated using the ΔΔ-Ct method using *RPLP0* gene expression as the normalisation control.

RNA Sequencing and Gene Set Enrichment Analysis

U87 spheroids were grown in static culture or in microfluidic culture for 7 days prior to RNA extraction as described above. Library preparation and sequencing using the Illumina NovaSeq 6000 platform were performed by Novogene Co Ltd. (Cambridge, UK). The HISAT2 algorithm was used for read alignment and FPKM calculated to estimate gene expression in each sample[29]. Gene expression data from the static cultured samples were used as the reference gene expression dataset. Differential gene expression analysis was performed using read counts obtained from gene expression analysis and the DESeq2 R package[30]. Gene expression change in microfluidic cultured spheroids compared to spheroids cultured in ULA plates were $\log_2$ transformed.

Calculated *p*-values were adjusted using the Benjamini and Hochberg method for controlling the false discovery rate (padj). Differentially expressed genes (pval < 0.05) with a gene symbol/ID annotation that were up- or down-regulated 1.5-fold ($\log_2$ fold change = ±0.585) were analysed using gene set enrichment analysis (GSEA) software[31, 32] (Broad Institute, Cambridge, MA, USA). Genes were ranked based on their $\log_2$ fold change (positive to negative). Ranked lists were then compared against the "Hallmark", "Gene Ontology - Biological Process", and "Kyoto Encyclopedia of Gene and Genes (KEGG) Pathway" curated gene-sets from the Molecular Signatures Database v6.2 (MSigDB, Broad Institute).

Results

Microfluidic chip structure and spheroid culture

The microfluidic chip used for spheroid growth was made from PMMA. Many microfluidic chips for cell/tissue culture are made from poly-di-methyl-siloxane (PDMS), however, PMMA is not affected by absorption of soluble proteins and is more resistant to solvents than PDMS. In addition, it has good thermal stability and insulation properties[33-35]. Compared to other thermoplastic materials, PMMA also allows for rapid fabrication due to its high mechanical strength and rigidity and is relatively

cheap[36]. This method of fabrication enabled the rapid production of versatile devices at a much lower cost than conventional techniques.

The microfluidic chip was a combination of four separate pieces (the inlet piece, the sample chamber, the tissue retaining piece and outlet piece (circular)) which are assembled using chloroform (**Fig 1**). The inlet has a diameter of 4 mm, which permits facile manipulation of spheroids. A sample chamber of a comparable size has been used previously to culture up to 4 spheroids, although this was in a glass horizontal device [28].

Shear stress caused by blood passing through vessels in tissues is a key physiological factor affecting the tumour microenvironment and has been proposed to affect proliferation, apoptosis, invasion, and metastasis of tumour cells[37]. At a flow rate of 2 µl/min it was calculated that the liquid flow over the spheroids was laminar, indicated by the Reynold number (Re) equalling 0.5×10^{-2}. Shear stress was calculated to be 4.9×10^{-5} dyne/cm^2 (calculations outlined in Supplementary Information).

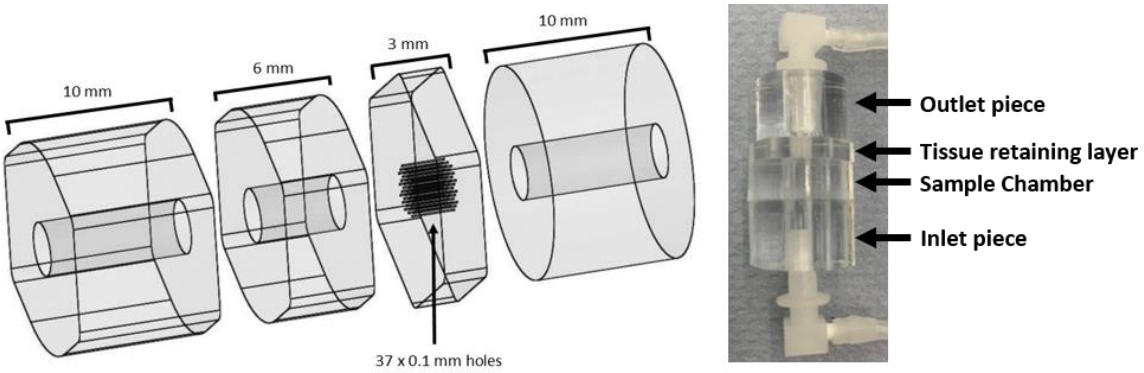

Figure 1. 3D schematic of the microfluidic chip
The hexagonal inlet layer is 10 mm thick; the sample chamber is 6 mm thick, the tissue retaining layer is 3 mm with 37 x 0.1 mm holes drilled to allow fluid flow through the device and the outlet layer is 10 mm thick.

Initially the integrity of spheroids formed by the GBM cell line U87 in microfluidic culture using the chip was assessed. Briefly, U87 cells were seeded in 96-well round-bottom ULA plates to allow spheroid formation. The spheroids were then transferred to the microfluidic chip and cultured under laminar flow at a flow rate of 2 µl/min. This flow rate has previously been used in a number of other devices with similar dimensions that we have developed[38, 39]. A comparison of the shape of U87 spheroids grown for 72 hours in parallel in static plate culture or microfluidic culture was then made. In static culture the spheroids were a uniform round shape with a compact structure. Spheroids in microfluidic culture kept their structure but generally appeared to become a little more oval in shape and appeared less compact (**Fig 2**).

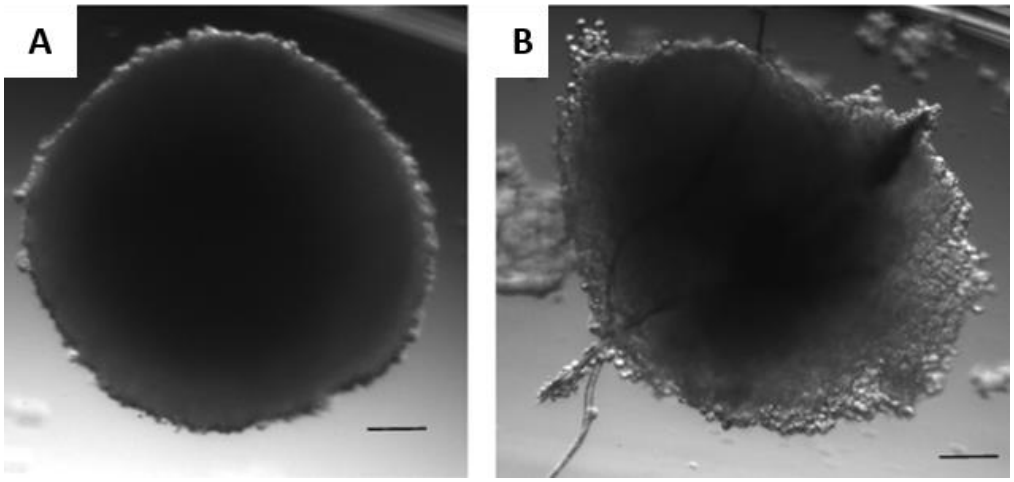

Figure 2. Light microscopy of U87 spheroids in static and microfluidic culture
Spheroids were cultured for 72hr in ULA plates (A) and in the microfluidic device (B). Scale bar: 100µm. Representative of 4 spheroids from two independent experiments.

Transcriptomic analysis of GBM spheroids grown in static culture and microfluidic culture

In order to understand what effect microfluidic culture has on spheroid growth and development at the gene expression level, RNA-sequencing was conducted on spheroids grown in both conditions. Differentially expressed genes between the two culture techniques was then assessed.

First, an experiment was conducted to determine the RNA yield from 12 spheroids at different time points of culture. Spheroids were cultured for 3 or 7 days in static and microfluidic culture followed by RNA extraction and quantification (**Fig 3a)**. In both conditions 7 day culture produced a higher RNA yield, likely due to there being more cells present after the longer time. This suggested that the cells were still proliferating between days 3 and 7 of culture. It was also observed that at 7 days of culture RNA yield was significantly higher from spheroids grown in microfluidic devices compared to static culture. This also suggested that cells in spheroids in the microfluidic devices are proliferating at a greater rate than cells in static culture. It was decided that for the RNA-sequencing analysis cells cultured for 7 days in static and microfluidic culture would be compared. This timeframe was chosen as we had demonstrated that cells were still in a proliferative state after 7 days of culture (data not shown) and gene expression patterns would be established for comparison after this duration of culture using both culture methods.

Differential gene expression analysis showed that 1565 genes were significantly upregulated whereas 1810 genes were significantly downregulated ($p<0.05$) at least 1.5 fold in spheroids grown in the microfluidic chip compared with those grown statically on a ULA plate, demonstrating that flow culture makes a significant difference to global gene expression patterns in spheroids (**Fig 3b**). Gene

Set Enrichment Analysis (GSEA) of differentially expressed genes (up- and down-regulated 1.5 fold with an adjusted p-value (padj) < 0.05) identified upregulation of genes associated with increased proliferation. For example, cell cycle processes, mitosis, and pro-proliferative oncogenic signalling pathways (e.g. E2F signalling, MTORC1 signalling and MYC signalling) (**Table 1**). These findings correlate with the observation that total RNA yield was higher in spheroids grown in microfluidic culture compared to static culture. There was also a pattern of downregulation of genes associated with cell adhesion (**Table 2**). This correlates with previous phenotypic observation of the spheroids grown in microfluidic culture, which appeared to be less compact and of a less uniform shape than spheroids grown in ULA plates (**Fig 2**).

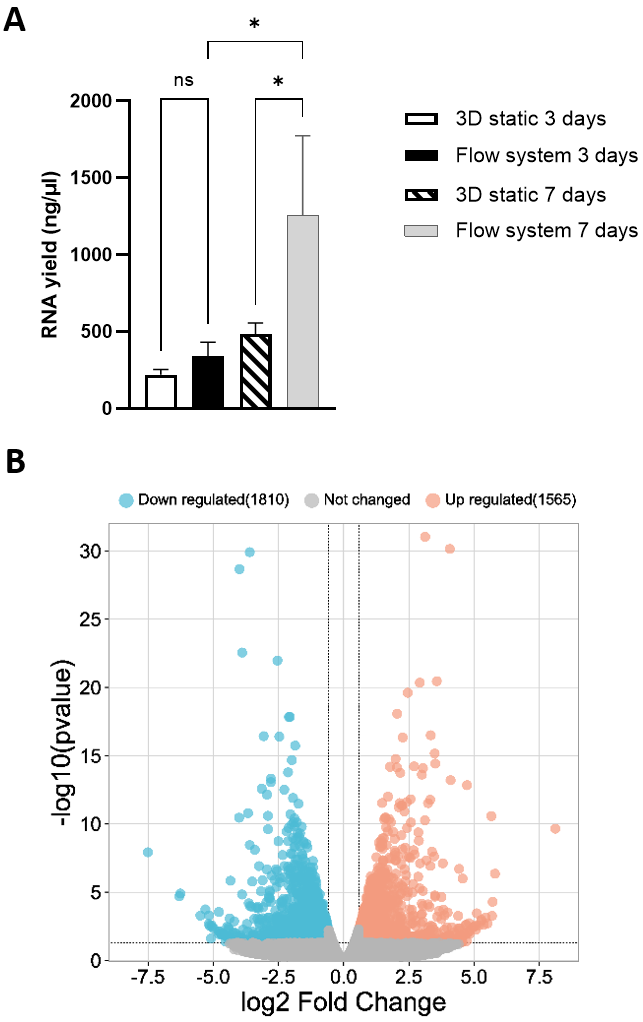

Figure 3 – Comparison of gene expression patterns of spheroids grown in static and microfluidic culture. *(A) Twelve U87 spheroids were grown in static or microfluidic culture for either 3 or 7 days followed by RNA extraction and quantification. The mean RNA concentration in ng/µl of each condition*

*and time point of 3 repeats ±SEM are shown, *p≤0.05.Twelve spheroids were subsequently grown for 7 days in microfluidic or static culture followed by RNA extraction and RNA-sequencing analysis. (B) Volcano plot of genes significantly (p<0.05) up-regulated (n=1565, red dots) or down-regulated (n=1810; blue dots) at least 1.5 fold in spheroids grown in microfluidic devices compared to static culture.*

Table 1. *Significantly enriched gene sets for genes significantly (padj<0.05) up-regulated at least 1.5 fold in spheroids grown in microfluidic culture compared to static culture.*

Hallmark Gene Set				
NAME	**SIZE**	**NES**	**NOM p-val**	**FDR q-val**
HALLMARK_E2F_TARGETS HALLMARK_E2F_TARGETS	57	4.57	>0.001	>0.001
HALLMARK_G2M_CHECKPOINT HALLMARK_G2M_CHECKPOINT	49	4.39	>0.001	>0.001
HALLMARK_MTORC1_SIGNALING	33	2.78	>0.001	>0.001
HALLMARK_UV_RESPONSE_UP	17	2.56	>0.001	>0.001
HALLMARK_MYC_TARGETS_V1	18	2.33	>0.001	0.001
HALLMARK_MITOTIC_SPINDLE	17	2.09	0.002	0.006
HALLMARK_TNFA_SIGNALING_VIA_NFKB	38	1.74	0.009	0.047
Gene Ontology - Biological Process Gene Set				
NAME	**SIZE**	**NES**	**NOM p-val**	**FDR q-val**
GOBP_CELL_CYCLE	166	4.91	>0.001	>0.001
GOBP_CHROMOSOME_ORGANIZATION	71	4.87	>0.001	>0.001
GOBP_MITOTIC_CELL_CYCLE_PROCESS	92	4.59	>0.001	>0.001
GOBP_MITOTIC_CELL_CYCLE	105	4.54	>0.001	>0.001
GOBP_DNA_METABOLIC_PROCESS	85	4.48	>0.001	>0.001
GOBP_CELL_CYCLE_PROCESS	122	4.40	>0.001	>0.001
GOBP_CELLULAR_RESPONSE_TO_DNA_DAMAGE_STIMULUS	67	3.88	>0.001	>0.001
GOBP_NEGATIVE_REGULATION_OF_CELL_CYCLE	47	3.85	>0.001	>0.001
GOBP_ORGANELLE_FISSION	57	3.79	>0.001	>0.001
GOBP_CELL_CYCLE_PHASE_TRANSITION	70	3.77	>0.001	>0.001
KEGG pathway gene set				
NAME	**SIZE**	**NES**	**NOM p-val**	**FDR q-val**
KEGG_CELL_CYCLE	24	2.44	>0.001	>0.001

Gene sets from the Hallmark, Gene Ontology – Biological Process KEGG pathway curated gene set database are shown. Gene sets are ranked by normalized enrichment score (NES). SIZE = number of differentially expressed genes enriched in the gene set. NOM p-val = nominal p-value, FDR q-val = false discover rate q-value. Only gene sets with an FDR q-val < 0.05 are shown. If more than 10 gene sets have and FDR q-val < 0.05 for a curated gene set database the top 10 most significantly enriched gene sets (according to NES) are shown.

Table 2. *Significantly enriched gene sets for genes significantly (padj<0.05) down-regulated at least 1.5 fold in spheroids grown in microfluidic culture compared to static culture.*

Hallmark Gene Set				
NAME	**SIZE**	**NES**	**NOM p-val**	**FDR q-val**
HALLMARK_EPITHELIAL_MESENCHYMAL_TRANSITION	54	-2.73	>0.001	>0.001
HALLMARK_INTERFERON_GAMMA_RESPONSE	30	-2.07	>0.001	0.016
HALLMARK_ALLOGRAFT_REJECTION	23	-1.92	0.013	0.034
Gene Ontology - Biological Process Gene Set				
NAME	**SIZE**	**NES**	**NOM p-val**	**FDR q-val**
GOBP_CELL_ADHESION	147	-3.48	>0.001	>0.001
GOBP_CELL_SUBSTRATE_ADHESION	39	-2.92	>0.001	0.001
GOBP_CELL_CELL_ADHESION	84	-2.66	>0.001	0.006
GOBP_ANTIGEN_PROCESSING_AND_PRESENTATION_OF_PEPTIDE_OR_POLYSACCHARIDE_ANTIGEN_VIA_MHC_CLASS_II	15	-2.65	>0.001	0.006
GOBP_CELL_CELL_ADHESION_VIA_PLASMA_MEMBRANE_ADHESION_MOLECULES	27	-2.61	>0.001	0.006
GOBP_ANTIGEN_PROCESSING_AND_PRESENTATION	18	-2.51	>0.001	0.01
GOBP_B_CELL_MEDIATED_IMMUNITY	18	-2.51	>0.001	0.01
GOBP_ANTIGEN_PROCESSING_AND_PRESENTATION_OF_EXOGENOUS_ANTIGEN	15	-2.39	>0.001	0.019
GOBP_IMMUNE_EFFECTOR_PROCESS	49	-2.38	>0.001	0.018
GOBP_CELL_JUNCTION_ORGANIZATION	51	-2.38	0.002	0.016
KEGG pathway gene set				
NAME	**SIZE**	**NES**	**NOM p-val**	**FDR q-val**
KEGG_ANTIGEN_PROCESSING_AND_PRESENTATION	16	-2.82	>0.001	>0.001
KEGG_SYSTEMIC_LUPUS_ERYTHEMATOSUS	19	-2.79	>0.001	>0.001
KEGG_LEISHMANIA_INFECTION	18	-2.71	>0.001	>0.001
KEGG_FOCAL_ADHESION	34	-2.65	>0.001	>0.001
KEGG_CELL_ADHESION_MOLECULES_CAMS	23	-2.57	>0.001	0.001
KEGG_ECM_RECEPTOR_INTERACTION	19	-2.47	0.001	0.003
KEGG_VIRAL_MYOCARDITIS	16	-2.02	0.007	0.033

Gene sets from the Hallmark, Gene Ontology – Biological Process KEGG pathway curated gene set database are shown. Gene sets are ranked by normalized enrichment score (NES). SIZE = number of differentially expressed genes enriched in the gene set. NOM p-val = nominal p-value, FDR q-val = false discover rate q-value. Only gene sets with an FDR q-val < 0.05 are shown. If more than 10 gene sets have and FDR q-val < 0.05 for a curated gene set database the top 10 most significantly enriched gene sets (according to NES) are shown.

Gene knockdown by siRNA mediated RNAi in spheroids grown in 2D culture, static spheroid culture and microfluidic spheroid culture.

To determine if the microfluidic device could be used for RNAi based functional genomic studies, the efficiency of *PRMT2* and *RAB21* gene knockdown by lipophilic transfection of target specific siRNAs was compared between U87 cells grown in 2D culture, static spheroid culture and microfluidic culture. *PRMT2* and *RAB21* were chosen as target genes due to being highly expressed in U87 cells and the fact they have previously been utilised as target genes in RNAi based studies in this cell line[11, 12].

Initially, experiments were done in 2D cell culture to establish the minimal concentration of siRNA required for efficient gene knockdown which would be used for subsequent comparison across all three culture systems. Briefly, U87 cells were transfected with 5, 12.5 and 25 nM of either *PRMT2* target siRNA (siPRMT2), *RAB21* target siRNA (siRAB21) or a non-targeting siRNA control (siSCR) and grown for 48 hours. RNA was extracted from the cells and qPCR analysis performed to determine the expression of *PRMT2* and *RAB21* in siPRMT2/siRAB21 transfected cells compared with siSCR transfected cells (**Fig 4**). Transfection with 5nM of target siRNA reduced *PRMT2* expression by 75.7% and *RAB21* expression by 86.3% respectively, which demonstrates efficient gene knockdown. There was no statistically significant difference in the efficiency of gene knockdown for either gene between the 3 siRNA concentrations. Therefore, for subsequent comparative experiments 5nM siRNA was used.

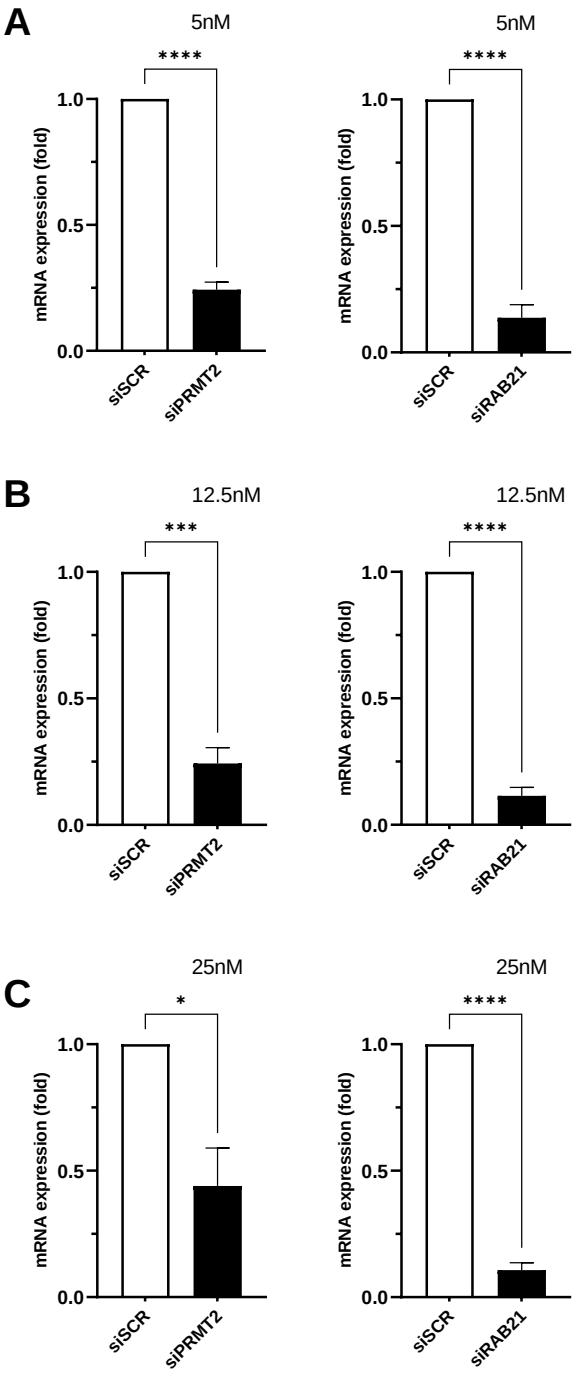

Figure 4. qPCR analysis of PRMT2 and RAB21 gene expression in U87 cells grown in 2D culture following siRNA mediated knockdown

*U87 cells were transfected with 5nM (A), 12.5nM (B) & 25nM (C) of either a non-silencing siRNA control (siSCR) or a PRMT2/RAB21 targeting siRNA (siPRMT2/siRAB21). Cells were grown for 48 hours followed by qPCR analysis. Data are presented as the mean relative fold change in gene expression compared to siSCR control of 3 repeats ±SEM, *p≤0.05; ***p≤0.001 and ****p≤0.0001. Statistical significance was evaluated using an unpaired t test*

For spheroids grown in static culture in ULA plates the efficiency of gene knockdown with 5nM siRNA was assessed at 48 and 72 hours post-transfection (**Fig 5**). *PRMT2* expression was significantly reduced 38.2% after 48 hours and 43.0% after 72 hours. There was no significant difference in knockdown efficiency between the two time points. *RAB21* gene expression was not significantly knocked down 48 hours post transfection but reduced by 59.0% 72 hours post transfection. For both *PRMT2* and *RAB21* the level of gene knockdown was enhanced at 72 hours compared to 48 hours, however neither reached the level of knockdown seen in 2D culture.

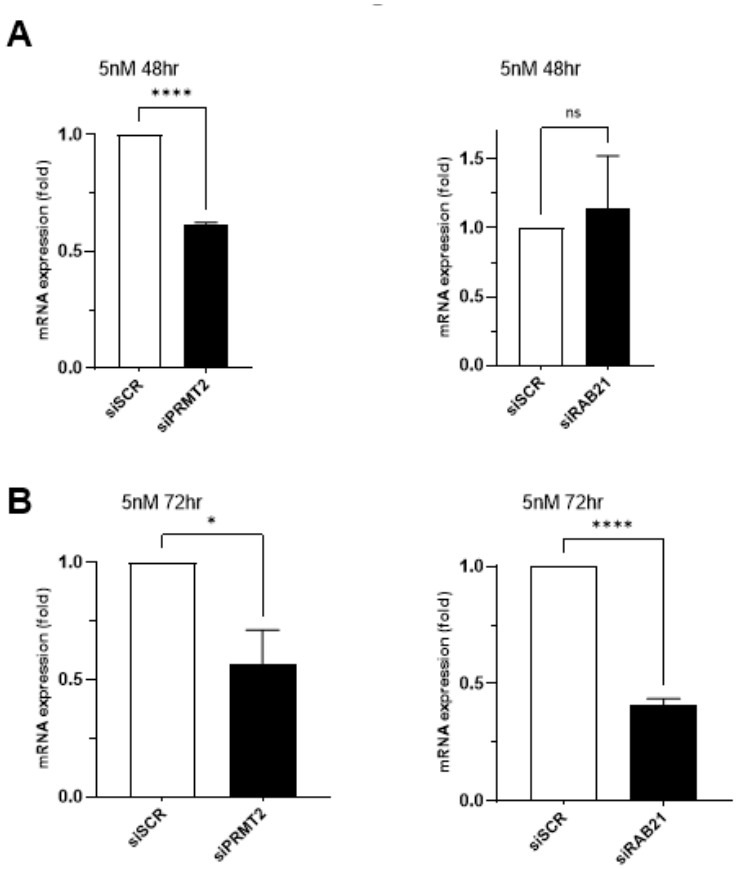

Figure 5. qPCR analysis of PRMT2 and RAB21 gene expression in U87 spheroids grown in static culture following siRNA mediated knockdown

*U87 spheroids were transfected with 5nM of either a non-silencing siRNA control (siSCR) or a PRMT2/RAB21 targeting siRNA (siPRMT2/siRAB21) and grown for either 48 hours (A) or 72 hours (B) followed by qPCR analysis. Data are presented as the mean relative fold change in gene expression compared to siSCR control of 3 repeats ±SEM, ns: not significant; *P ≤0.05; **P ≤ 0.01 and **** P≤ 0.0001. Statistical significance was evaluated using an unpaired t test.*

For knockdown in microfluidic culture, spheroids were transfected with 5nM siRNA and grown for 96 hours (**Fig 6a**). Subsequent qPCR analysis showed that *PRMT2* expression did not reduce compared to siSCR transfected cells, and *RAB21* expression reduced only 37% compared to siSCR transfected cells. Both results indicated a diminished knockdown efficiency in the flow system compared to static culture. A second microfluidic transfection protocol was tested whereby fresh transfection mixture

was administered to the cells every 24 hours of the 96 hour transfection (**Fig 6b**). This was done to try and provide an opportunity for the optimal concentration of siRNA to enter the cells over the time course of the experiment, due to the potential this was being reduced because of the flowing nature of the culture setup. This resulted in a significant reduction in *PRMT2* expression of 26.33%, however this was not at the same efficiency seen for static spheroid culture. Interestingly, *RAB21* expression was also reduced (19.67%), but not to the same efficiency as the single dose siRNA transfection protocol.

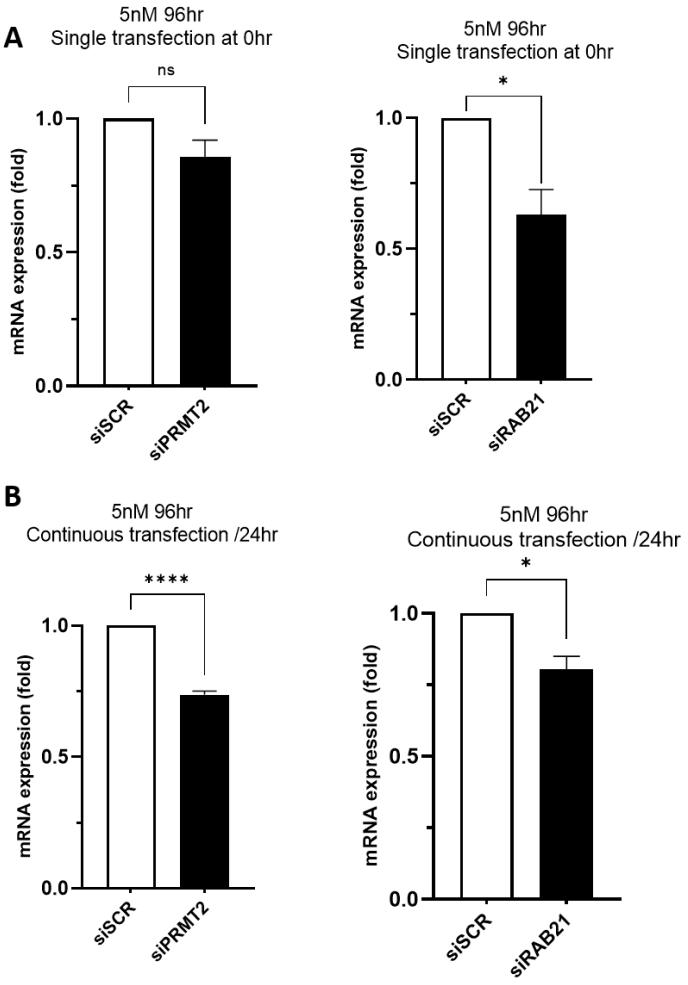

Figure 6. qPCR analysis of PRMT2 and RAB21 gene expression in U87 spheroids grown in microfluidic culture following siRNA mediated knockdown

*U87 spheroids were transfected with 5nM of either a non-silencing siRNA control (siSCR) or a PRMT2/RAB21 targeting siRNA (siPRMT2/siRAB21) and grown for either 96 hours followed by qPCR analysis. siRNA was either administered as a single transfection at the beginning of the experiment (A) or as a repeat transfection every 24 hours (B) Data are presented as the mean relative fold change in gene expression compared to siSCR control of 3 repeats ±SEM, ns: not significant, **** P≤ 0.0001 and *P ≤0.05 Statistical significance was evaluated using an unpaired t test.*

Discussion

A key tool for novel cancer therapeutic target identification and validation is genetic manipulation of proposed targets in cancer cell line models. This is particularly relevant when specific inhibitors have not yet been developed for the proposed target and the only way to investigate their function in cancer cells is via gene knockdown or overexpression. An inherent limitation of such gene function studies, however, is that the cancer cell line models often used have limited translational relevance and, therefore, the effects seen in them are not replicated *in vivo*. This has been highlighted as a particular problem for GBM[15].

3D spheroid cultures of cancer cells have been shown to have gene expression and phenotypic profiles which more closely resemble *in vivo* cancer tissue than cells grown in 2D monolayers[18-20]; however, limitations remain due to the cells often not being cultured in a physiologically relevant environment. Microfluidic culture of cancer cell spheroids and cancer tissue has overcome some of these limitations as cells are exposed to laminar flow shear stress that replicates the tumour microenvironment as well as a constant flow of nutrients with simultaneous removal of waste products, which mimics human physiology[21, 22, 38-40]. This study aimed to investigate whether gene knockdown could be achieved under microfluidic culture and, therefore, whether RNAi based target validation studies could utilise this more translationally relevant cell culture system.

We have used a reliable and robust microfluidic culture device which allows viable growth of GBM U87 spheroids. We demonstrated, via transcriptomic analysis, that spheroids grown on the microfluidic device upregulated gene-sets associated with a proliferative phenotype when compared with spheroids grown in static (non-flowing) culture. This suggested that microfluidic culture promoted growth of the spheroids compared to static culture, which was supported by the fact that the yield of RNA extracted from spheroids grown in the microfluidic device was significantly higher than spheroids grown for the same amount of time in ULA plates. Increased proliferation of spheroids grown in microfluidic culture compared to static culture has previously been demonstrated for other cell types, potentially due to the constant renewal of nutrients and removal of waste products, which, in static culture, can acidify culture media causing a growth inhibitory effect[41, 42].

Alongside upregulation of pro-proliferative genes there was downregulation of genes associated with cell adhesion. This was accompanied by the observation that spheroids grown in microfluidic culture had a slightly less compact appearance and were more oval in shape compared to the uniform round appearance of spheroids grown in static culture. The ellipsoid appearance of spheroids grown in microfluidic culture has been observed before for spheroids derived from bladder cancer patient derived xenografts (PDX), with the ellipsoid spheroids recapitulating patterns of drug response and

resistance of the PDXs grown *in vivo*[43]. Changes in shape of the spheroid may reflect loss of expression of genes associated with cell adhesion that may suggest a transition to a more invasive or aggressive phenotype of cells within the spheroids[44, 45]. Downregulation of cell adhesion molecules accompanied by increased motility has been seen previously in microfluidic culture of cancer spheroids, indicating a link between flow conditions and elevated invasive phenotypes[46].

In relation to gene knockdown in the different culture systems, we observed that *RAB21* and *PRMT2* knockdown was most efficient in 2D culture compared to static spheroid culture, and that knockdown was more efficient in static spheroid culture compared to microfluidic spheroid culture. Reduced knockdown efficiency in spheroid culture compared to 2D monolayer culture is a well-known phenomenon. This is likely due to the lipid molecules carrying the siRNA being less able to penetrate the 3D spheroid mass compared to 2D monolayer culture together with the fact that there is a much lower surface area to volume ratio of cells exposed to siRNA in these two models[47]. This ultimately results in reduced transfection efficiency. Despite this, at a relatively low siRNA concentration (5 nM), knockdown of gene expression by approximately 50% was seen for both genes in static spheroid culture. In microfluidic culture, this was reduced to approximately 25% for *PRMT2* and 40% for *RAB21*. The reduction in knockdown efficiency may be due to the flowing nature of the siRNA delivery, meaning that cells are not exposed to the lipid molecules carrying the siRNA for sufficient time to allow transfection to occur. This could potentially be counteracted by an increase in siRNA concentration and is something that should be explored further. In addition, alternative methods of siRNA delivery could be tested. For example, nanoparticle delivery of siRNA has been shown to increase transfection efficiency into cells[48-50].

Despite the sub-optimal knockdown efficiency in the flowing system we have demonstrated that gene knockdown is possible in microfluidic culture. The level of knockdown observed may not be sufficient to cause a biological effect for every target gene investigated, but for some targets this level of knockdown could be utilised for study of gene function in cancer cells. Microfluidic culture is also able to maintain tissue *ex vivo* in a viable state[23, 38-40]. The fact the chip described in this study was able to be used for gene knockdown in spheroids opens up the possibility of similar studies to be conducted in patient tissue samples, which would again increase the translational impact of target validation study using this culture model. The model has been used to demonstrate analysis of multiple cancer relevant phenotypes in tissues following drug treatment, including cell proliferation and cell death as well as analysis of protein expression[51]. Further optimisation and investigation of alternative siRNA transfection techniques should therefore be pursued to make use of the microfluidic cell culture system for in-depth target gene functional studies using RNAi.

Acknowledgements

This research was supported by the University of Hull

Conflict of Interest

The authors declare no conflict of interest.

Supplementary Information

Supplementary Table S1: Primers used for RT-qPCR analysis

Gene symbol	Strand	Primer sequence (5'–3')
PRMT2	F	CCCCACATCTCAAAAAGTTG
	R	AAGATATGCACACTGCTTTC
RAB21	F	AAGGATGATAGAAACAGCAC
	R	CATCAATAATCTGTACACCTCG
	R	GTCATCAAAAGAGACCGTTG
RPLP0	F	GGAGAAACTGCTGCCTCATCATA
	R	GGAAAAAGGAGGTCTTCTCG

Calculation of Reynold number (Re)

Reynold number formula: $Re = \rho.u.d/\mu$ where:

ρ = Density of the medium (kg/m^3) = 1007 kg/m^3

u = Velocity of the liquid in the channel (m/s) = Calculated below

d = Diameter of the microchannel of the chip (m) = 4 mm = 4 x 10^{-3} m

μ = Dynamic viscosity (Ns/m^2) = 9.4 x 10^{-4} Ns/m^2

Calculation of the velocity (u):

Relation between fluid velocity and the flow rate: Q = A.u

Q = flow rate (m^3/s) = 2 µl/min = 3.33 10^{-11} m^3/s

A = Area (m^2) = $\pi (d/2)^2$ = 1.25 x 10^{-5} m^2

Q = A.u → u = Q / A = 2.6 x 10^{-6} m/s

Reynold number numerical calculation

Re = 0.5 x 10^{-2}

Calculation of shear stress (τ)

$\tau = 32\ \mu\ Q/\ \pi\ d^3 = (32 \times 0.94 \times 10^{-3} \times 3.33 \times 10^{-11}\ m^3/s)/\ \pi \times (4 \times 10^{-3} m)^3$

$= 4.9\ 10^{-6}\ N/m^2 = 4.9\ 10^{-5}\ dyne/cm^2$

τ = Shear Stress (N/m^2)

μ = viscosity of the medium (DMEM with 10% FBS)

$= 0.94\ cP = 9.4 \times 10^{-4}\ N.s/m^2$

($1\ cP = 0.001\ Ns/m^2$)

Q= flow rate = 2µl/min = $3.33\ 10^{-11}\ m^3/s$

d= diameter of the microchannel of the chip = 4mm = $4.0 \times 10^{-3} m$

References

1. D. N. Louis, A. Perry, P. Wesseling, D. J. Brat, I. A. Cree, D. Figarella-Branger, C. Hawkins, H. K. Ng, S. M. Pfister, G. Reifenberger, R. Soffietti, A. von Deimling and D. W. Ellison, Neuro Oncol **23** (8), 1231-1251 (2021).
2. S. Lapointe, A. Perry and N. A. Butowski, Lancet **392** (10145), 432-446 (2018).
3. O. Rominiyi, A. Vanderlinden, S. J. Clenton, C. Bridgewater, Y. Al-Tamimi and S. J. Collis, Br J Cancer **124** (4), 697-709 (2021).
4. I. Spiteri, G. Caravagna, G. D. Cresswell, A. Vatsiou, D. Nichol, A. Acar, L. Ermini, K. Chkhaidze, B. Werner, R. Mair, E. Brognaro, R. G. W. Verhaak, G. Sanguinetti, S. G. M. Piccirillo, C. Watts and A. Sottoriva, Ann Oncol **30** (3), 456-463 (2019).
5. A. L. V. Alves, I. N. F. Gomes, A. C. Carloni, M. N. Rosa, L. S. da Silva, A. F. Evangelista, R. M. Reis and V. A. O. Silva, Stem Cell Res Ther **12** (1), 206 (2021).
6. A. F. Tamimi and M. Juweid, in *Glioblastoma*, edited by S. De Vleeschouwer (Brisbane (AU), 2017).
7. S. J. Bagley, S. Kothari, R. Rahman, E. Q. Lee, G. P. Dunn, E. Galanis, S. M. Chang, L. B. Nabors, M. S. Ahluwalia, R. Stupp, M. P. Mehta, D. A. Reardon, S. A. Grossman, E. P. Sulman, J. H. Sampson, S. Khagi, M. Weller, T. F. Cloughesy, P. Y. Wen and M. Khasraw, Clin Cancer Res **28** (4), 594-602 (2022).
8. H. M. Martineau and I. T. Pyrah, Toxicol Pathol **35** (3), 327-336 (2007).
9. S. E. Mohr, J. A. Smith, C. E. Shamu, R. A. Neumuller and N. Perrimon, Nat Rev Mol Cell Biol **15** (9), 591-600 (2014).
10. P. Diehl, D. Tedesco and A. Chenchik, Drug Discov Today Technol **11**, 11-18 (2014).
11. J. Ge, Q. Chen, B. Liu, L. Wang, S. Zhang and B. Ji, Cell Mol Biol Lett **22**, 30 (2017).
12. F. Dong, Q. Li, C. Yang, D. Huo, X. Wang, C. Ai, Y. Kong, X. Sun, W. Wang, Y. Zhou, X. Liu, W. Li, W. Gao, W. Liu, C. Kang and X. Wu, Nat Commun **9** (1), 4552 (2018).
13. D. Jones, L. Wilson, H. Thomas, L. Gaughan and M. A. Wade, Cancers (Basel) **11** (8) (2019).
14. L. J. Bilton, C. Warren, R. M. Humphries, S. Kalsi, E. Waters, T. Francis, W. Dobrowinski, P. Beltran-Alvarez and M. A. Wade, Cancers (Basel) **14** (14) (2022).
15. K. Aldape, K. M. Brindle, L. Chesler, R. Chopra, A. Gajjar, M. R. Gilbert, N. Gottardo, D. H. Gutmann, D. Hargrave, E. C. Holland, D. T. W. Jones, J. A. Joyce, P. Kearns, M. W. Kieran, I. K. Mellinghoff, M. Merchant, S. M. Pfister, S. M. Pollard, V. Ramaswamy, J. N. Rich, G. W. Robinson, D. H. Rowitch, J. H. Sampson, M. D. Taylor, P. Workman and R. J. Gilbertson, Nat Rev Clin Oncol **16** (8), 509-520 (2019).
16. M. Kapalczynska, T. Kolenda, W. Przybyla, M. Zajaczkowska, A. Teresiak, V. Filas, M. Ibbs, R. Blizniak, L. Luczewski and K. Lamperska, Arch Med Sci **14** (4), 910-919 (2018).
17. S. A. Langhans, Front Pharmacol **9**, 6 (2018).

18. S. Ghosh, G. C. Spagnoli, I. Martin, S. Ploegert, P. Demougin, M. Heberer and A. Reschner, J Cell Physiol **204** (2), 522-531 (2005).
19. P. A. Kenny, G. Y. Lee, C. A. Myers, R. M. Neve, J. R. Semeiks, P. T. Spellman, K. Lorenz, E. H. Lee, M. H. Barcellos-Hoff, O. W. Petersen, J. W. Gray and M. J. Bissell, Mol Oncol **1** (1), 84-96 (2007).
20. J. M. Lee, P. Mhawech-Fauceglia, N. Lee, L. C. Parsanian, Y. G. Lin, S. A. Gayther and K. Lawrenson, Lab Invest **93** (5), 528-542 (2013).
21. S. J. Hachey and C. C. W. Hughes, Lab Chip **18** (19), 2893-2912 (2018).
22. L. Wan, C. A. Neumann and P. R. LeDuc, Lab Chip **20** (5), 873-888 (2020).
23. F. Olubajo, S. Achawal and J. Greenman, Transl Oncol **13** (1), 1-10 (2020).
24. Y. H. V. Ma, K. Middleton, L. D. You and Y. Sun, Microsyst Nanoeng **4** (2018).
25. A. G. Niculescu, C. Chircov, A. C. Birca and A. M. Grumezescu, Int J Mol Sci **22** (4) (2021).
26. J. Wu, Z. Y. Zhu, Z. W. Fan, Y. Chen, R. Y. Yang and Y. Li, Neural Regen Res **17** (2), 362-369 (2022).
27. S. Lee, S. Kim, D. J. Koo, J. Yu, H. Cho, H. Lee, J. M. Song, S. Y. Kim, D. H. Min and N. L. Jeon, ACS Nano **15** (1), 338-350 (2021).
28. T. Collins, E. Pyne, M. Christensen, A. Iles, N. Pamme and I. M. Pires, Biomicrofluidics **15** (4), 044103 (2021).
29. A. Mortazavi, B. A. Williams, K. McCue, L. Schaeffer and B. Wold, Nat Methods **5** (7), 621-628 (2008).
30. S. Anders and W. Huber, Genome Biol **11** (10), R106 (2010).
31. V. K. Mootha, C. M. Lindgren, K. F. Eriksson, A. Subramanian, S. Sihag, J. Lehar, P. Puigserver, E. Carlsson, M. Ridderstrale, E. Laurila, N. Houstis, M. J. Daly, N. Patterson, J. P. Mesirov, T. R. Golub, P. Tamayo, B. Spiegelman, E. S. Lander, J. N. Hirschhorn, D. Altshuler and L. C. Groop, Nat Genet **34** (3), 267-273 (2003).
32. A. Subramanian, P. Tamayo, V. K. Mootha, S. Mukherjee, B. L. Ebert, M. A. Gillette, A. Paulovich, S. L. Pomeroy, T. R. Golub, E. S. Lander and J. P. Mesirov, Proc Natl Acad Sci U S A **102** (43), 15545-15550 (2005).
33. J. Liu, C. F. Chen, C. W. Tsao, C. C. Chang, C. C. Chu and D. L. DeVoe, Anal Chem **81** (7), 2545-2554 (2009).
34. C. W. Tsao, Micromachines (Basel) **7** (12) (2016).
35. E. Gencturk, S. Mutlu and K. O. Ulgen, Biomicrofluidics **11** (5), 051502 (2017).
36. A. B. Sozmen and A. A. Yildiz, Microfluid Nanofluid **25** (8) (2021).
37. Q. Huang, X. Hu, W. He, Y. Zhao, S. Hao, Q. Wu, S. Li, S. Zhang and M. Shi, Am J Cancer Res **8** (5), 763-777 (2018).
38. A. Riley, V. Green, R. Cheah, G. McKenzie, L. Karsai, J. England and J. Greenman, BMC Cancer **19** (1), 259 (2019).
39. R. Kennedy, D. Kuvshinov, A. Sdrolia, E. Kuvshinova, K. Hilton, S. Crank, A. W. Beavis, V. Green and J. Greenman, Sci Rep **9** (1), 6327 (2019).
40. S. M. Hattersley, C. E. Dyer, J. Greenman and S. J. Haswell, Lab Chip **8** (11), 1842-1846 (2008).
41. H. H. Tsai, K. C. Yang, M. H. Wu, J. C. Chen and C. L. Tseng, Int J Mol Sci **20** (16) (2019).
42. N. Dadgar, A. M. Gonzalez-Suarez, P. Fattahi, X. Hou, J. S. Weroha, A. Gaspar-Maia, G. Stybayeva and A. Revzin, Microsyst Nanoeng **6**, 93 (2020).
43. P. Gheibi, S. Zeng, K. J. Son, T. Vu, A. H. Ma, M. A. Dall'Era, S. A. Yap, R. W. de Vere White, C. X. Pan and A. Revzin, Sci Rep **7** (1), 12277 (2017).
44. V. Gkretsi and T. Stylianopoulos, Front Oncol **8**, 145 (2018).
45. M. Janiszewska, M. C. Primi and T. Izard, J Biol Chem **295** (8), 2495-2505 (2020).
46. Y. L. Huang, Y. Ma, C. Wu, C. Shiau, J. E. Segall and M. Wu, Sci Rep **10** (1), 9648 (2020).
47. R. G. Morgan, A. C. Chambers, D. N. Legge, S. J. Coles, A. Greenhough and A. C. Williams, Sci Rep **8** (1), 7952 (2018).
48. J. Xu, M. Gu, L. Hooi, T. B. Toh, D. K. H. Thng, J. J. Lim and E. K. Chow, Nanoscale **13** (38), 16131-16145 (2021).

49. E. Oner, M. Kotmakci, A. M. Baird, S. G. Gray, B. Debelec Butuner, E. Bozkurt, A. G. Kantarci and S. P. Finn, J Nanobiotechnology **19** (1), 71 (2021).
50. F. Mainini and M. R. Eccles, Molecules **25** (11) (2020).
51. A. Barry, S. F. Samuel, I. Hosni, A. Moursi, L. Feugere, C. J. Sennett, S. Deepak, S. Achawal, C. Rajaraman, A. Iles, K. C. Wollenberg Valero, I. S. Scott, V. Green, L. F. Stead, J. Greenman, M. A. Wade and P. Beltran-Alvarez, Lab Chip **23** (11), 2664-2682 (2023).